A Simulation-Based Study on the Influence of the Impact Velocity on the Structural Deformation, Stress, and Cabin Intrusion of Passenger Vehicles

Le Xuan Cuong
Institute of Forensic Science, Ministry of Public, Hanoi, Vietnam
lexuancuong.ifs@gmail.com (corresponding author)

Received: 28 October 2025 | Revised: 26 November 2025, 6 December 2025, 9 December 2025, and 15 December 2025 | Accepted: 16 December 2025

 DOI: https://doi.org/10.48084/etasr.15829

ABSTRACT

The deformation and failure process of automobile components begins at the moment of impact. This complex physical phenomenon is influenced by numerous factors, many of which are random. This report presents a mathematical simulation of a moving vehicle colliding with a fixed barrier. The modeling process uses HyperMesh for preprocessing and Radioss for numerical computation to simulate the formation, deformation, and failure of vehicle components. The results of the numerical simulation are then compared with experimental data for analysis and evaluation. Recommendations are proposed to solve the problem of determining the vehicle's speed immediately before impact. These recommendations can serve as a reference for traffic accident investigations in Vietnam. The results show that as vehicle speed increases from 56 km/h to 80 km/h, the maximum displacement rises from 20 mm to over 120 mm and the maximum stress increases from 3,200 MPa to over 6,500 MPa, surpassing the material's strength limit. Contact energy increases nonlinearly, from 2.54×10^6 Nm at 55 km/h to 9.00×10^6 Nm at 80 km/h, reflecting the influence of plastic folding and strain rate effects. At speeds exceeding 70 km/h, the footwell, brake pedal area, and vehicle doors experience severe intrusion, which significantly reduces passenger protection capacity.

Keywords-frontal collision; numerical simulation; stress–strain; energy absorption; cabin intrusion

I. INTRODUCTION

Traffic accidents pose a continuous challenge for modern transportation systems, resulting in significant human and economic losses. Authors in [1] examined driver-related and accident-specific factors in Iraq, while authors in [2] analyzed crash patterns in Saudi Arabia to identify primary causes, underscoring the importance of understanding crash dynamics and vehicle safety to improve and minimize structural damage, through experimental tests and numerical simulations. Despite improvements in automotive technology, which include optimizing engine systems to reduce emissions [3, 4] and accelerating the transition to electric vehicles and lightweight materials [5, 6], developing a strong structure that minimizes damage and protects passengers remains challenging, underscoring the need for continued research into deformation mechanisms and energy absorption under various impact conditions. Authors in [7] studied vehicle collision dynamics through experimental and analytical approaches based on rigid-body impact mechanics, proposing computational methods to reconstruct vehicle crashes and estimate energy dissipation and impact severity. Authors in [8] used the finite element method to simulate frontal car crashes at different speeds and ANSYS to analyze stress-strain distribution and evaluate the strength of various body structures and composite materials, improving passenger safety and structural integrity. Authors in [9] presented a method for reconstructing pre- and post-impact vehicle kinematics based on PC-Crash simulations. This method enables the accurate determination of collision parameters and supports the validation of accident reconstruction. Authors in [10] developed a finite element model of the THOR crash test dummy head and neck system, comparing simulation results with physical tests to confirm the reliability of FE-based dummy modeling in industrial crash analyses. Authors in [11] explored the strength of Fiber-Reinforced Composites (FRCs), when combined with aluminum frames. Authors in [12] analyzed the severity of rear-end collisions using a regression model to find human and structural factors influencing crash results. Authors in [13] evaluated the effectiveness of traffic safety measures in Latin America and the Caribbean, emphasizing the role of vehicle design standards in reducing fatalities. Authors in [14] examined the relationship between rear-end collision risk, vehicle speed, inter-vehicle distance, and road conditions. Authors in [15] optimized the front longitudinal beam using finite element analysis and dynamic drop testing, achieving

higher energy absorption with reduced vehicle mass. Automotive crash safety is a global challenge requiring the integration of mechanical design, materials engineering, technology, and intelligent support systems. In Vietnam, research primarily focuses on crash simulation and general kinematic analysis. However, detailed quantitative assessments, such as the influence of velocity on deformation behavior, stress distribution, and cabin intrusion, are limited. This study's novel contribution is the development of a detailed finite element model of the 2017 Chevrolet Silverado 1500 consisting of over 2.03 million mesh elements. This model is used to evaluate the relationship between collision velocity and the vehicle structure's key mechanical characteristics, including deformation, maximum stress, contact energy, and cabin intrusion. This research identifies the velocity threshold at which the vehicle frame continues to provide effective occupant protection and proposes design recommendations for energy absorption zones to enhance passenger safety in high-speed collisions. These findings are highly relevant for developing countries such as Vietnam.

II. METHODOLOGY

A. Conservation of Energy Equation

In collision simulation problems, the total energy of a mechanical system can be broken down into several distinct components. For mechanical impacts, the primary forms of energy are kinetic, internal, rotational, thermal, and acoustic energy. The general relationship among these components is:

$$E_{kinetic} = E_{internal} + E_{rotational} + E_{thermal} + E_{acoustic} \quad (1)$$

where $E_{kinetic}$ is the initial kinetic energy before impact, $E_{internal}$ is the deformation energy, $E_{rotational}$ is the rotational kinetic energy of the body, $E_{thermal}$ is the thermal energy generated during the collision, and $E_{acoustic}$ is the acoustic energy produced during the collision. In this collision simulation, the total simulation time is 0.15 s. Therefore, energy components, such as rotational, thermal, and acoustic energies, cannot be accurately evaluated throughout the entire impact process and can be neglected. This simplification is justified because the materials involved in the collision do not exhibit physical properties that produce significant thermal or acoustic effects. In this case, these minor energy components can be neglected while retaining the primary components: kinetic and internal energies. The total energy equation can be simplified as:

$$E_{kinetic} = E_{internal} \quad (2)$$

where:

$$E_{kinetic} = \frac{1}{2}mv^2 \quad (3)$$

$$E_{internal} = \frac{1}{2}\int \sigma.\varepsilon.dv = \frac{1}{2}K_{eq}\delta_{max}^2 \quad (4)$$

where σ is the stress at the corresponding point (Pa), ε is the strain at the corresponding point, m is the mass of the body involved in the collision, and v is the velocity of the body at the moment of impact. Simplifying the energy equation reduces computational complexity while maintaining simulation accuracy when rotational, thermal, and acoustic energies have negligible effects on the collision process. This approach is essential in simulation practice because it reduces computation time and improves efficiency in applications such as automotive design, crash safety analysis, and impact behavior investigation in materials research.

B. Conservation of Momentum Equation

Under inelastic collision conditions, the principle of energy conservation implies that the colliding masses possess equivalent converted kinetic energy from the onset of motion until maximum deformation occurs, just before separation. According to the theorem of linear momentum conservation:

$$m_1v_1 + m_2v_2 = m_1v'_1 + m_2v'_2 \quad (5)$$

where m_1 is the mass of the colliding vehicle, m_2 is the mass of the barrier, v_1 is the initial velocity of the first body before impact, v_2 is the initial velocity of the second body before impact, v'_1 is the velocity of the first body after impact and v'_2 is the velocity of the second body after impact. In the special case where the obstacle is stationary ($v_2 = 0$), the equation is simplified as:

$$m_1v_1 = m_1v'_1 + m_2v'_2 \quad (6)$$

Additionally, this study focuses on evaluating the use of composite deformation depth (C), which is determined by calculating the deformation depth according to:

$$C = \frac{\frac{C_m}{2} + \frac{C_n}{2} + \sum_{i=m+1}^{n-1} C_i}{n-m} \quad (7)$$

where C_m, C_n represent the deformation depths at the two boundaries (the starting and ending points) of the deformation zone; C_i represents the deformation depth at the intermediate points; and m and n are the indices of the first and last measurement points, respectively.

C. Impulse Absorption Equation

$$I = \int F(t)dt \quad (8)$$

where I is the impulse (N.s) and $F(t)$ is the time-dependent impact force. The time integration indicates the total effect of the force throughout the collision process.

III. ESTABLISHMENT OF THE COLLISION SIMULATION MODEL

The 2017 Chevrolet Silverado 1500, shown in Figure 1, was selected as the subject of this collision simulation study for its technical characteristics and performance. The chassis structure was meshed and modeled using the RADIOSS solver for simulation analysis. Approximately 2.03 million elements were generated through the HyperMesh software, with a mesh size ranging from 5 mm to 10 mm, as presented in Table I. The simulation was configured as a full-frontal impact with a collision angle of 0°, meaning that the vehicle's direction of travel was perpendicular to a rigid wall. The vehicle's mass was set to its actual curb weight, and the wall was assumed to be perfectly rigid and unreformable, so the vehicle's entire kinetic energy would be dissipated through structural deformation. Two impact velocities were examined — 64.4 km/h and 80 km/h — to evaluate the vehicle's energy absorption performance and the level of protection offered to the

passengers under more severe crash conditions. In this configuration, the initial energy of the system was computed and assumed to be distributed primarily to the front energy-absorbing regions. The passenger compartment functions as a protected zone, and its structural integrity must be preserved.

TABLE I. REFERENCE OVERALL VEHICLE DIMENSIONS

Parameter	Value	Unit
Wheelbase	3,644	mm
Overall width	2,060	mm
Overall height	1,923	mm
Ground clearance	226	mm
Curb weight	2,372	kg

The study performed frontal collision simulations at impact velocities of 56 km/h and 80 km/h to analyze vehicle frame deformation and occupant protection capabilities. The 56 km/h velocity was selected in accordance with the IIHS Moderate Overlap Frontal Test standard to ensure comparability with international benchmarks. The 80 km/h scenario was added to reflect real-world, high-speed traffic conditions, such as those observed on expressways in Vietnam. This scenario allowed for the evaluation of structural load-bearing capacity and stability limits under more severe conditions.

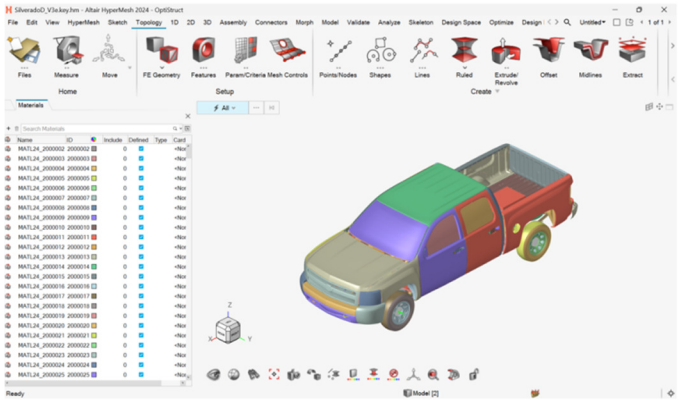

Fig. 1. Vehicle simulation model.

In the simulation, the vehicle collides directly with a rigid wall, and the boundary conditions are configured to closely resemble real-world situations. The analysis focuses on:

- The deformation level of the cabin area.
- The intrusion/displacement of critical structural components, such as the A-pillar and floor panel.

Various forms of energy, including kinetic, internal, contact, and total energy, were monitored during the simulation process to validate the model's physical accuracy. The results demonstrated in Figure 2 indicate that:

- The total energy (orange curve) remains conserved with negligible fluctuations, confirming that the model does not experience numerical energy loss.
- The kinetic energy (red curve) gradually decreases during the collision, reflecting the dissipation of motion energy.
- The internal energy (blue curve) increases correspondingly, indicating that energy is being absorbed through the structural deformation of the vehicle frame, which is the primary mechanism ensuring occupant protection.
- The contact energy (green curve) has small, stable values consistent with direct frontal impact against a rigid wall.

The balanced transformation of kinetic energy into internal energy, along with the conservation of total energy, confirms that the simulation model is stable and reliable. This provides a solid basis for subsequent analyses of deformation behavior and crash safety.

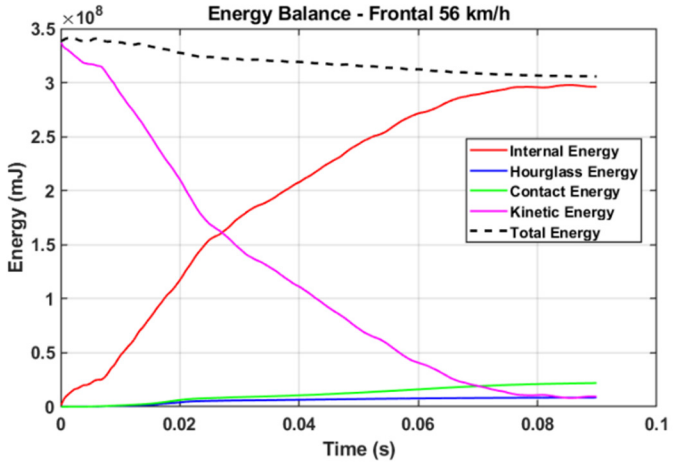

Fig. 2. Verification of energy conservation in the collision simulation model.

IV. RESULTS AND DISCUSSION

Figures 3 and 4 present the simulation results, showing the relationship between impact velocity, maximum displacement, and peak stress in the vehicle structure. As velocity increases, displacement and stress rise sharply, reflecting a clear linear correlation between initial kinetic energy and structural deformation. Specifically, at 56 km/h, the maximum displacement is approximately 20 mm, and the peak stress is about 3,200 MPa. This indicates that the structure effectively maintains its protective integrity. As velocity increases to 65 km/h and 70 km/h, the maximum displacement rises to around 70 mm and 90 mm, respectively. Correspondingly, peak stress increases to approximately 4,300 MPa and 5,000 MPa. At 80 km/h, the maximum displacement exceeds 120 mm, and the peak stress surpasses 6,500 MPa. This approaches or exceeds the yield strength of structural steel and indicates that the vehicle frame undergoes severe deformation, approaching instability and significantly compromising the passenger safety zone. This is consistent with the fundamental principle of collision mechanics that kinetic energy is proportional to the square of velocity. Therefore, even a small increase in speed results in a substantial increase in displacement and stress levels. These findings confirm that the simulation accurately reproduces the underlying physical mechanisms and demonstrate that the vehicle frame provides effective protection only under standard impact conditions (56 km/h).

Beyond 70–80 km/h, there is a critically high risk of passenger compartment intrusion and loss of safety.

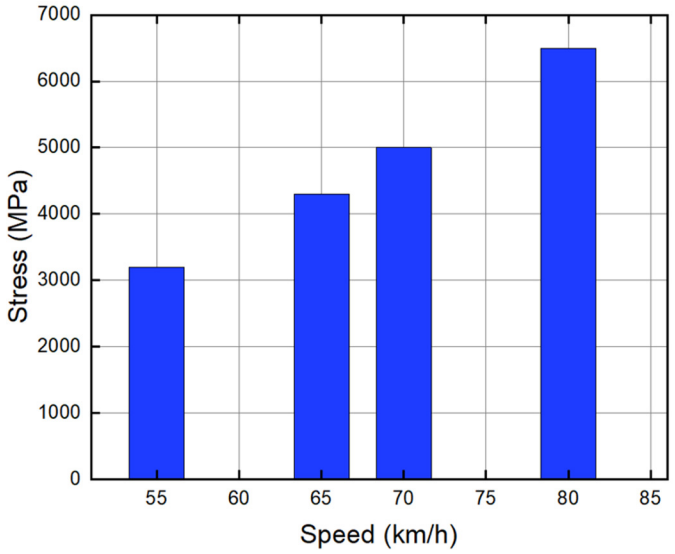

Fig. 3. Relationship between impact velocity and maximum structural displacement of the vehicle.

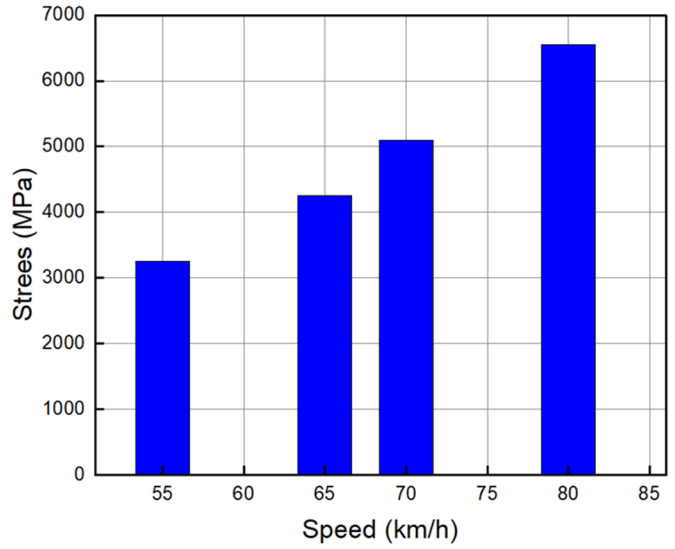

Fig. 4. Relationship between impact velocity and maximum structural stress of the vehicle.

Figure 5 shows the relationship between the impact velocity (km/h) and the contact energy (Nm) of the vehicle structure. As the impact velocity increases, the contact energy rises significantly. Specifically, the contact energy is approximately 2.54×10^6 Nm at 55 km/h, 5.79×10^6 Nm at 65 km/h (an increase of over 128%), 8.19×10^6 Nm at 70 km/h (41.5% higher), and 9.00×10^6 Nm at 80 km/h (nearly a 10% increase). This trend aligns with the fundamental principle of collision mechanics, where kinetic energy is proportional to the square of velocity. However, the observed increase in contact energy exceeds the theoretical prediction, especially within the velocity range of 65–70 km/h. This is due to a change in the structural energy absorption mechanism. At lower speeds, energy is primarily dissipated through localized deformation. At higher speeds, however, plastic folding, deformation propagation, and strain-rate effects become dominant, which results in enhanced energy dissipation capacity. At velocities between 70 km/h and 80 km/h, the contact energy approaches saturation, indicating that the structure has nearly exhausted its deformation capacity and is approaching its stability limit.

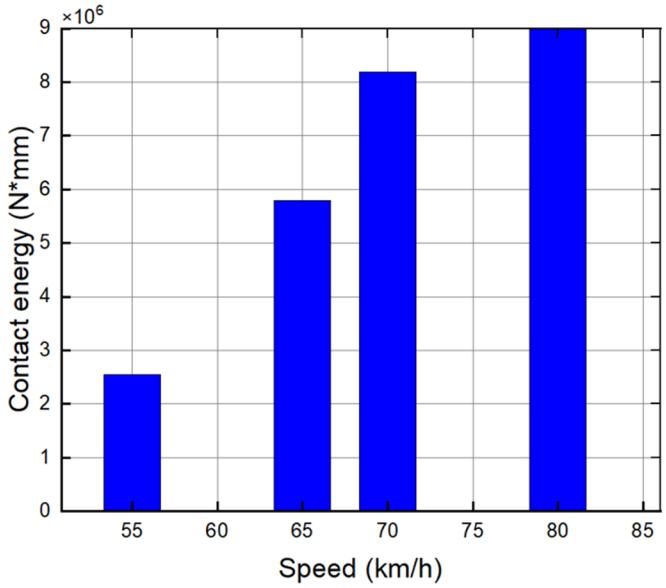

Fig. 5. Relationship between impact velocity and contact energy of the vehicle during collision.

Figure 6 illustrates the measured intrusion of the driver's compartment at various impact velocities ranging from 56 km/h to 80 km/h. The vehicle demonstrates excellent crash protection at 56 km/h and 64.4 km/h, with nearly all measurement points positioned within the GOOD safety zone (0–5 cm intrusion).

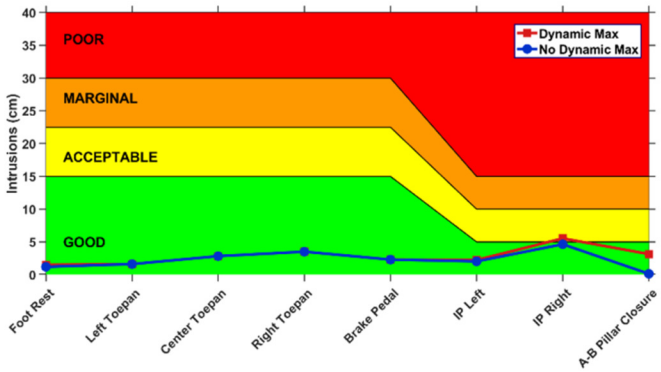

Fig. 6. Comparison of driver compartment intrusion at different impact velocities.

The footwell and brake-pedal regions record displacements of approximately 3.2 cm and 3.8 cm, respectively, confirming the front frame's high stiffness and efficient energy absorption.

These low values indicate sufficient survival space and minimal risk of lower-limb injury. As the velocity increases to 70 km/h, the intrusion values increase significantly. The footrest shows an intrusion of 9.8 cm, and the console and brake pedal areas show intrusions of 10.6 cm and 11.2 cm, respectively. These values are still within the ACCEPTABLE zone (light yellow), but they indicate the onset of localized deformation. The door panel records an intrusion of 8.9 cm, suggesting a partial loss of side-frame rigidity. At 80 km/h, intrusion rises sharply across all monitored locations. The footrest reaches 16.8 cm, the console region reaches approximately 15.2 cm, and the brake pedal reaches approximately 14.7 cm. All of these values fall into the marginal zone (orange). Door intrusion increases to 12.3 cm, indicating that the A/B-pillar assembly has exceeded its elastic deformation limit. These values correspond to a roughly 45–55% reduction in survival space compared to the standard 56 km/h condition. This confirms that, above 70 km/h, the cabin structure can no longer maintain optimal load-bearing performance, and the risk of serious driver injury rises significantly. In summary, as the impact velocity increases from 56 km/h to 80 km/h, the vehicle transitions from an excellent safety condition to a moderate protection level. In this level, the footwell, brake pedal, instrument panel, and door frame become the primary zones of structural compromise, which poses a high risk of serious injury to the driver.

V. CONCLUSIONS

This paper provides a detailed, quantitative crash dataset for a large, body-on-frame vehicle. Most existing studies focus on passenger cars with monocoque structures; however, analyses of heavy pickup trucks with separate frames, like the Silverado 1500, are limited despite their distinct load-transfer mechanisms, energy-absorption behavior, and cabin-intrusion characteristics. Selecting the Silverado 1500 allows this study to clarify how body-on-frame construction specifically influences plastic collapse, deformation propagation, and load-path instability during full-frontal impacts, at crash velocities relevant to Vietnamese traffic conditions. The results provide a quantitative assessment of how impact velocity governs deformation progression, stress distribution, and energy absorption behavior. As velocity increases from 56 km/h to 80 km/h, the structure transitions from localized bending to extensive plastic collapse. The maximum displacement rises from 20 mm to over 120 mm, and the peak frame stress increases from 3,200 MPa to over 6,500 MPa. A critical transition region is identified at 65–70 km/h, where the energy-absorption mechanism shifts, and large-scale plastic propagation begins to dominate the structural response. The findings demonstrate that cabin intrusion is minimal below 65 km/h, but increases sharply at higher speeds, reaching 12–17 cm in the footwell and dashboard areas. These results identify the velocity threshold at which the structural load path becomes unstable and the occupant compartment is compromised. They also establish a clear correlation between external deformation markers and internal failure modes, providing valuable reference data for structural optimization and accident reconstruction.

REFERENCES

[1] R. Abdulla, B. Qader, and K. Sdiq, "Traffic Accident Traits and Driver Characteristics Implication on Road Accidents using Descriptive Analysis: A Cross Sectional Study in Sulaymaniyah, Iraq," *Engineering, Technology & Applied Science Research*, vol. 13, no. 2, pp. 10372–10376, Apr. 2023, https://doi.org/10.48084/etasr.5669.

[2] N. K. Al-Shammari and S. M. H. Darwish, "In-depth Sampling Study of Charactersitics of Vehcile Crashes in Saudi Arabia," *Engineering, Technology & Applied Science Research*, vol. 9, no. 5, pp. 4724–4728, Oct. 2019, https://doi.org/10.48084/etasr.2939.

[3] N. X. Khoa and O. Lim, "The Internal Residual Gas and Effective Release Energy of a Spark-Ignition Engine with Various Inlet Port–Bore Ratios and Full Load Condition," *Energies*, vol. 14, no. 13, Jan. 2021, Art. no. 3773, https://doi.org/10.3390/en14133773.

[4] N. X. Khoa, N. T. Nghia, V. H. Quan, and N. A. Ngoc, "The Effects of EGR and Oxygen Content on the GCI Engine Performance Under Two-Injection Modes and Fueled Biodiesel Blends," *Arabian Journal for Science and Engineering*, vol. 49, no. 8, pp. 10859–10866, Aug. 2024, https://doi.org/10.1007/s13369-023-08477-2.

[5] L.-T. Hieu, N. X. Khoa, and O. Lim, "An Investigation on the Effects of Input Parameters on the Dynamic and Electric Consumption of Electric Motorcycles," *Sustainability*, vol. 13, no. 13, Jan. 2021, Art. no. 7285, https://doi.org/10.3390/su13137285.

[6] L. T. Hieu, N. X. Khoa, and O. T. Lim, "An investigation on the effective performance area of the electric bicycle with variable key input parameters," *Journal of Cleaner Production*, vol. 321, Oct. 2021, Art. no. 128862, https://doi.org/10.1016/j.jclepro.2021.128862.

[7] G. Albert and T. Lotan, "Exploring the impact of 'soft blocking' on smartphone usage of young drivers," *Accident Analysis & Prevention*, vol. 125, pp. 56–62, Apr. 2019, https://doi.org/10.1016/j.aap.2019.01.031.

[8] D. Bendjaballah, M. Sahli, and T. Barrière, "Modeling and numerical simulation of car frontal crash test using finite element method," *Journal of Materials Science: Materials in Engineering*, vol. 20, no. 1, p. 108, Aug. 2025, https://doi.org/10.1186/s40712-025-00326-4.

[9] Y. G. Zhang, J. M. Xu, T. F. Zou, and Y. Liu, "A Method for Reconstructing Vehicle - Vehicle Impact Accidents Based on Pc-Crash," *Applied Mechanics and Materials*, vol. 641–642, pp. 799–804, 2014, https://doi.org/10.4028/www.scientific.net/AMM.641-642.799.

[10] J. Canha, F. DiMasi, Y. Tang, M. Haffner, and T. Shams, "Development of a Finite Element Model of the Thor Crash Test Dummy," *SAE Transactions*, vol. 109, pp. 258–268, 2000.

[11] "Crashworthiness design issues for lightweight vehicles," in *Materials, Design and Manufacturing for Lightweight Vehicles*, Woodhead Publishing, 2021, pp. 433–470.

[12] S. A. Mohamed, Kishta. Mohamed, and H. A. Al-Harthi., "Investigating Factors Affecting the Occurrence and Severity of Rear-End Crashes," *Transportation Research Procedia*, vol. 25, pp. 2098–2107, Jan. 2017, https://doi.org/10.1016/j.trpro.2017.05.403.

[13] K. Bhalla and K. Gleason, "Effects of vehicle safety design on road traffic deaths, injuries, and public health burden in the Latin American region: a modelling study," *The Lancet Global Health*, vol. 8, no. 6, pp. e819–e828, June 2020, https://doi.org/10.1016/S2214-109X(20)30102-9.

[14] P. Zhao and C. Lee, "Assessing rear-end collision risk of cars and heavy vehicles on freeways using a surrogate safety measure," *Accident Analysis & Prevention*, vol. 113, pp. 149–158, Apr. 2018, https://doi.org/10.1016/j.aap.2018.01.033.

[15] Q. Q. Li, E. Li, T. Chen, L. Wu, G. Q. Wang, and Z. C. He, "Improve the frontal crashworthiness of vehicle through the design of front rail," *Thin-Walled Structures*, vol. 162, May 2021, Art. no. 107588, https://doi.org/10.1016/j.tws.2021.107588.